

Dayside global ionospheric response to the major interplanetary events of October 29–30, 2003 “Halloween Storms”

A. J. Mannucci,¹ B. T. Tsurutani,¹ B. A. Iijima,¹ A. Komjathy,¹ A. Saito,² W. D. Gonzalez,³ F. L. Guarnieri,³ J. U. Kozyra,⁴ and R. Skoug⁵

Received 12 September 2004; accepted 21 March 2005; published 4 May 2005.

[1] We demonstrate extreme ionospheric response to the large interplanetary electric fields during the “Halloween” storms that occurred on October 29 and 30, 2003. Within a few (2–5) hours of the time when the enhanced interplanetary electric field impinged on the magnetopause, dayside total electron content increases of $\sim 40\%$ and $\sim 250\%$ are observed for the October 29 and 30 events, respectively. During the Oct 30 event, $\sim 900\%$ increases in electron content above the CHAMP satellite (~ 400 km altitude) were observed at mid-latitudes (± 30 degrees geomagnetic). The geomagnetic storm-time phenomenon of prompt penetration electric fields is a possible contributing cause of these electron content increases, producing dayside ionospheric uplift combined with equatorial plasma diffusion along magnetic field lines to higher latitudes, creating a “daytime super-fountain” effect. **Citation:** Mannucci, A. J., B. T. Tsurutani, B. A. Iijima, A. Komjathy, A. Saito, W. D. Gonzalez, F. L. Guarnieri, J. U. Kozyra, and R. Skoug (2005), Dayside global ionospheric response to the major interplanetary events of October 29–30, 2003 “Halloween Storms,” *Geophys. Res. Lett.*, 32, L12S02, doi:10.1029/2004GL021467.

1. Introduction

[2] The ionospheric response to changes in solar wind conditions has been the subject of concerted study for several decades [Blanc and Richmond, 1980; Prolss, 1997; Buonsanto, 1999; Richmond and Lu, 2000; Fuller-Rowell et al., 1997]. The complex interaction of the solar wind, magnetosphere, thermosphere and ionosphere causes dynamical changes over a variety of spatial and temporal scales. In this paper we report very large hemispheric-scale daytime changes in plasma structure of the Earth’s ionosphere during the extreme interplanetary (geomagnetic storm) events of October 29–30, 2003 (“Halloween storms”). A factor contributing to the TEC increases may be daytime eastward-directed electric fields penetrating promptly from high to low latitudes, as has been reported previously but primarily for dusk to midnight local times [Fejer, 2002; Tanaka and Ohtaka, 1996; Vlasov et al., 2003; Fejer and Scherliess, 1997; Greenspan et al., 1991].

¹Jet Propulsion Laboratory, California Institute of Technology, Pasadena, California, USA.

²Department of Geophysics, Kyoto University, Kyoto, Japan.

³Instituto de Pesquisas Espaciais, São José dos Campos, Brazil.

⁴Department of Atmospheric, Oceanic and Space Sciences, University of Michigan, Ann Arbor, Michigan, USA.

⁵Los Alamos National Laboratory, Los Alamos, New Mexico, USA.

[3] We use Global Positioning System receiver data acquired from ground-based receivers and a low Earth-orbiting receiver. Space-borne receivers using upward viewing antennas measure the electron content above the satellite altitude (CHAMP at 400 km altitude). CHAMP measurements along with DMSP ion drift measurements suggest that large ionospheric uplift occurs due to electric fields.

2. Observations

[4] Figure 1 shows data associated with two interplanetary coronal mass ejections (ICMEs) plus their associated shocks that were detected by the ACE spacecraft upstream of the Earth on October 29 and 30, 2003, including proton speed, temperature, density, and magnetic fields from ACE, and *Dst* index values. The ICMEs causing the magnetic storms were related to X-class solar flares that occurred on October 28 and October 29, 2003 [see Tsurutani et al., 2005].

[5] The first geomagnetic storm of interest is associated with an abrupt *Dst* decrease at ~ 1400 UT on October 29. B_z initially has a magnitude of $+8$ nT but continues to turn steadily southward, reaching a value of -30 nT at 1910 UT. This B_z southward turning, part of a magnetic cloud [Skoug et al., 2004], combined with solar wind velocities in the range 1200–2100 km/sec, causes a geomagnetic storm and peak *Dst* excursion of -350 nT recorded at 0125 UT on October 30. The shock of a second ICME occurs at ~ 1650 UT on October 30. The strong southward magnetic field at and just after the shock causes another geomagnetic storm that commences at 1845 UT (during the recovery phase of the previous storm). This last storm is the most intense, with peak *Dst* of -390 nT at 2315 UT on October 30.

[6] The main topic of this paper are these B_z southward events followed by unusually large daytime ionospheric responses as measured by ionospheric total electron content (TEC) data obtained from Global Positioning System (GPS) receivers. Using techniques mentioned extensively in the literature [Mannucci et al., 1998, 1999] a dual-frequency GPS receiver can measure the total electron content of the ionosphere/plasmasphere system between the receiver and satellite, with high precision (0.01 TECU is typical, 1 TECU = 10^{16} el/m²) and reasonable accuracy ($\sim 1-3$ TECU).

[7] Vertical TEC data derived from a global network of ~ 100 GPS receivers are plotted in Figure 2 for several days leading up to and through the geomagnetic storm periods of October 29–30, 2003. An obliquity function is used to estimate the vertical TEC from the slant TEC measurements obtained above 10 degrees elevation angle: we assume that

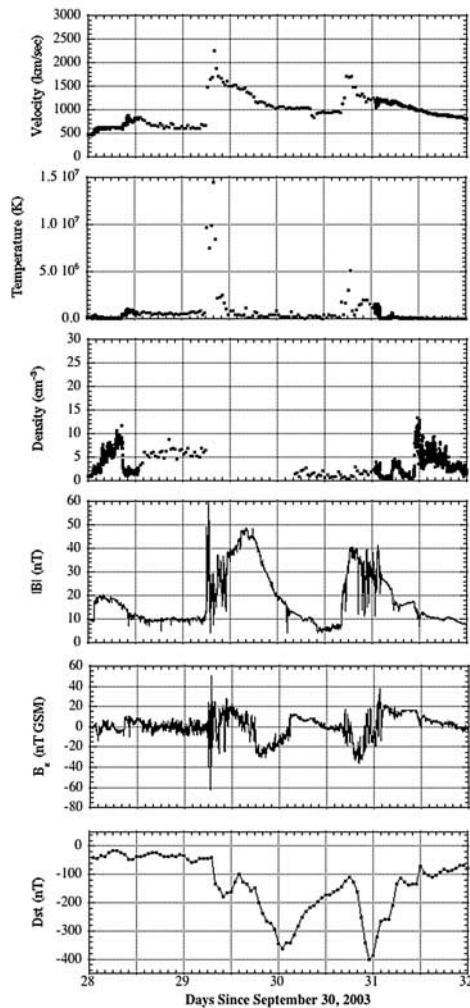


Figure 1. The interplanetary event of late October 2003. The interplanetary data were obtained by the ACE spacecraft, including the proton speed in km/sec, the proton temperature (K), proton density (cm^{-3}), and magnetic field magnitude (nT). The magnetic field component B_z is plotted for GSM coordinates. The southward- B_z events on October 29 and 30 lead to large geomagnetic storms and ring current increases as measured by the Dst index.

the ionosphere occupies a spherical slab of uniform vertical electron density between 450 and 650 km altitude. The latitude and longitude at which the ground-to-satellite line-of-sight intersects the ionosphere is computed using a spherical shell at 450 km altitude.

[8] The TEC measurements in the local time range 1400–1600 LT and magnetic latitude range ± 40 degrees (IGRF) [Richmond, 1995] were averaged every 30-minutes of Universal Time (UT), to examine TEC behavior at low to middle latitudes. The resultant time series of average vertical TEC versus UT is plotted along with the computed interplanetary electric field (IEF), derived from the product $V_x \times B_z$ (GSM coordinates) measured by the plasma and magnetic field instruments onboard the ACE spacecraft [Skoug et al., 2004]. The IEF data is offset by the propagation time from ACE to the magnetospheric bow shock and is only plotted for values where the product $V_x \times B_z$ is positive.

[9] Also plotted in magenta in Figure 2 is the average TEC plus its standard deviation, computed from the scatter of all vertical TEC data contributing to the average value. The observed TEC increases of $\sim 50\%$ – 250% (after the larger IEF increase) are much larger than the day-to-day variability observed prior to the IEF increases. The number of points contributing to the averages ranged from 50 to 600, depending on UT, as the number of sites within the relevant local time varied.

[10] Variability of TEC with time shown in Figure 2 is likely due to two factors: variability of the ionosphere itself, and the fact that the GPS receiver distribution varies with longitude. Even if the ionospheric TEC were not changing, the latitude sampling of the receivers used to compute the average is changing with UT, thereby changing the locations at which TEC is measured. Ionospheric features that exhibit latitudinal structure will change the average as a function of time. Despite these sources of uncertainty, a strong correlation is observed between enhanced TEC and B_z south (enhanced interplanetary electric field), which is clearly distinguished from the preceding quiet-time data. The local time/latitude range used to compute the average was chosen to emphasize effects within a broad daytime, low latitude region.

[11] Daytime observations of the TEC above the CHAMP satellite altitude of 400 km on October 30 were available from the upward-viewing GPS antenna, plotted in Figure 3. Slant measurements obtained above 40 degrees elevation are scaled to estimate vertical TEC above the satellite altitude, using a geometric factor derived by assuming the plasma occupies a spherical shell ionosphere of uniform density and 700 km thickness above the CHAMP altitude. There

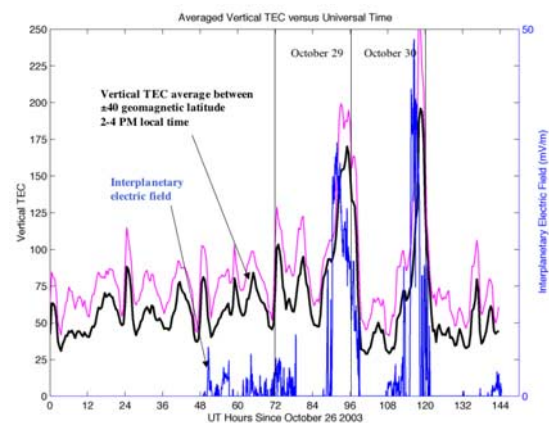


Figure 2. The average of estimated vertical ionospheric total electron content from the ground GPS network is plotted for several days leading up to and including the Halloween 2003 storms. The average (solid black line) is calculated over the range ± 40 degrees apex latitude, for local times between 14–16 LT. The interplanetary electric field as measured by the ACE spacecraft ($v_x \times B_z$, GSM coordinates) is plotted in blue, delayed according to the velocity measured by ACE (Figure 1), assuming a distance between ACE and the magnetopause of 1.4×10^6 km. The TEC added to its standard deviation computed for all measurements at a given epoch is also shown (solid magenta line).

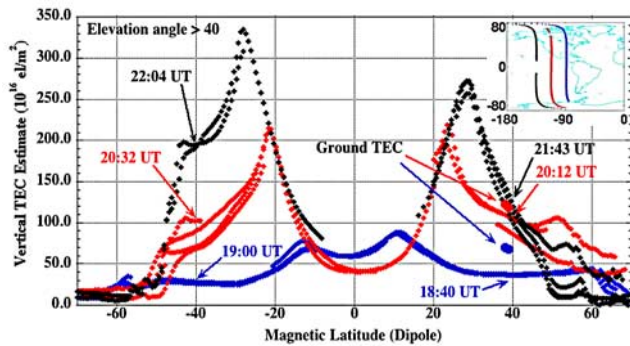


Figure 3. The supersatellite integrated electron content (IEC) as measured by the CHAMP spacecraft is shown just prior (blue trace) and after (red and black traces) the onset of the interplanetary event of October 30 (see Figure 1). The different sets of points for each trace correspond to IEC measured towards the different GPS satellites at each epoch, which are all used to estimate vertical TEC directly above the CHAMP satellite altitude of 400 km, using an elevation angle cut-off of 40 degrees to reduce the error in the vertical IEC estimation procedure. The local time of the CHAMP orbit ranges from 1230–1330 LT for latitudes within ± 60 degrees. Points missing near the anomaly trough are due to the elevation angle cut-off. The universal times of the -40 and $+40$ degree latitude cross-over points are shown for each trace. Also shown in the upper right are the geographical locations of the traces. Total electron content averages from ground data near to the CHAMP ground track are shown as round dots.

are generally several points at a given epoch (seen as multiple traces for a single color) because there can be more than one GPS satellite in view of CHAMP at elevations greater than 40 degrees. The separate traces generally agree, except for the red traces between 40 and 60 degrees latitude, which differ because of the azimuth of the raypaths to the GPS satellites: the lower TEC values are associated with a satellite being tracked in the northwest direction versus northeast/east-directed azimuths for the higher TEC values. These traces differ because of horizontal TEC gradients in the vicinity of the satellite.

[12] Three daytime ascending passes are shown in Figure 3, one pass before the larger interplanetary B_z south event of October 30, and two that occurred afterwards. Prior to the interplanetary event (blue markers), the CHAMP latitudinal profile shows the typical “two-peak” structure similar to an undisturbed equatorial anomaly [Hanson and Moffett, 1966].

[13] The first post-onset pass (red markers), starting at 2012 UT, measures a vastly increased TEC above CHAMP, up to 200 TECU, with the peaks farther apart. This trace begins approximately 1.25 hours after the onset of the sustained IMF southward- B_z event at 1900 UT. Inspection of ground-based TEC data from North America (not shown) indicate that temporal changes, not longitudinal gradients, are responsible for the differences between the pre-onset and first post-onset pass. The TEC increases still further to ~ 350 TECU in the southern hemisphere approximately 1.5 hours later (black markers, second pass after southward B_z). The twin peak features previously identified

as an equatorial anomaly now appear at mid-latitudes (± 28 degrees). The ionospheric TEC above CHAMP altitudes has increased by an order of magnitude (900%) at mid-latitudes (-30° geomagnetic). Part of the difference between this pass and the previous one may be due to longitudinal TEC gradients, which have begun to build up on the North American west coast, according to ground-based TEC (not shown).

[14] We have plotted select vertical TEC from ground-based GPS receivers in North America (red and blue dots at 38 and 39 degrees geomagnetic latitude), for measurements located within ± 6 minutes and within ± 3 degrees longitude of the CHAMP ground track location at the latitude shown. Prior to the interplanetary event (blue dots), the integrated electron content above CHAMP comprises a smaller fraction of the TEC compared to after the interplanetary event (red dots), reinforcing the conclusion that plasma uplift has occurred.

3. Interpretation and Discussion

[15] Figure 2 suggests a strong correlation between increased IEF and significant dayside increases in TEC (positive ionospheric storm). A large IEF event that occurred in November of 2001 was studied by Tsurutani *et al.* [2004], where analysis of multiple data sets led to the conclusion that prompt penetration electric fields contributed to the TEC increase and uplift. Another source of storm-time electric fields at equatorial latitudes is the thermospheric disturbance dynamo [Blanc and Richmond, 1980], but, as discussed by Richmond and Lu [2000], such daytime electric fields are generally of opposite sign to those reported here. Prompt penetration electric fields tend to be eastward during daytime before shielding has built up [Nopper and Carovillano, 1978]. A daytime eastward electric field raises low latitude plasma upward due to $\mathbf{E} \times \mathbf{B}$ drift, so that more plasma resides at higher altitudes where recombination rates decrease, while additional plasma continues to be generated by solar illumination, resulting in a net increase of electrons above 400 km, consistent with the CHAMP data. We refer to this large TEC enhancement as the “daytime super-fountain effect” associated with magnetic storms, described further by Tsurutani *et al.* [2004]. Tanaka and Ohtaka [1996] describe a dusk “super-fountain” associated with prompt penetration electric fields that applies to that local time range. High-altitude plasma can take hours to recombine, so we cannot infer from our data the duration of the penetrating electric field. That will require detailed modeling.

[16] To further assess our hypothesis that daytime eastward electric fields contribute to the large TEC increases, we used data from the DMSP satellite (F13) at 1745 local time, which shows evidence of enhanced electric fields between geomagnetic latitudes of -10 and 10 degrees. The drift velocity at DMSP altitude (840 km) is predominantly negative during the days October 25–30 2003, except for three distinct periods when the drift velocity becomes significantly upward (>70 m/sec): October 29 at 0616 UT and at 1951–2313 UT; and during October 30 1941–2118 UT. The times of these large vertical drift velocities correspond to the periods of southward B_z shown in Figure 1.

[17] The daytime plasma uplift has potentially important ionospheric/atmospheric effects. Following Figure 3 and assuming an average of 200 TECU (2×10^{14} Oxygen ions/cm²) over 0.25 of the Earth's surface is elevated to a height of 800 km in two hours, the rate of work done by the solar wind corresponds to 3.8 Giga-watts (this is only a small fraction of the solar wind ram energy). The total potential energy is 2.7×10^{13} Joules.

[18] If the entire ionosphere is uplifted to heights of 800 km or more, two prominent effects may occur. With the reduction of plasma density at ~ 250 km altitude, ion-neutral drag will be substantially reduced and will change the neutral wind system at the equatorial region. Secondly the uplifted heavy ions (O₂⁺, NO⁺) will diffuse down magnetic field lines to midlatitudes leading to global (dayside) mixing.

4. Conclusions

[19] The dramatic TEC increase due to plasma uplift during geomagnetic storms is one of the most dramatic consequences of magnetosphere-thermosphere-ionosphere coupling. Transport of plasma poleward, and possibly uplift at mid-latitudes, causes major mid-latitude plasma increases that may contribute to the extreme TEC gradients at mid-latitudes that have been reported as part of TEC plumes associated with subauroral electric fields [e.g., Foster et al., 2002]. If prompt penetration electric fields are playing a role, a better understanding of magnetosphere-ionosphere coupling, including the role of shielding, will clarify our understanding of extreme space weather events over a wide range of latitudes.

[20] **Acknowledgments.** Portions of the research for this paper were performed at the Jet Propulsion Laboratory, California Institute of Technology under contract with NASA. Work at Los Alamos was performed under the auspices of the U. S. Department of Energy with support from the NASA ACE program. We thank the ACE SWEPAM instrument team and the ACE Science Center for providing the ACE data. We gratefully acknowledge the Center for Space Sciences at the University of Texas at Dallas and the US Air Force for making available the DMSP drift velocity data. One of the authors (AJM) wishes to thank the anonymous referees for their useful suggestions.

References

- Blanc, M., and A. D. Richmond (1980), The ionospheric disturbance dynamo, *J. Geophys. Res.*, *85*, 1669–1686.
- Buonsanto, M. J. (1999), Ionospheric storms—A review, *Space Sci. Rev.*, *88*, 563–601.
- Fejer, B. G. (2002), Low latitude storm time ionospheric electrodynamics, *J. Atmos. Sol. Terr. Phys.*, *64*, 1401–1408.
- Fejer, B. G., and L. Scherliess (1997), Empirical models of storm time equatorial zonal electric fields, *J. Geophys. Res.*, *102*, 24,047–24,056.
- Foster, J. C., P. J. Erickson, A. J. Coster, J. Goldstein, and F. J. Rich (2002), Ionospheric signatures of plasmaspheric tails, *Geophys. Res. Lett.*, *29*(13), 1623, doi:10.1029/2002GL015067.
- Fuller-Rowell, T. M., M. V. Codrescu, R. G. Roble, and A. D. Richmond (1997), How does the thermosphere and ionosphere react to a geomagnetic storm?, in *Magnetic Storms, Geophys. Monogr. Ser.*, vol. 98, edited by B. T. Tsurutani et al., pp. 203–225, AGU, Washington, D. C.
- Greenspan, M. E., C. E. Rasmussen, W. J. Burke, and M. A. Abdu (1991), Equatorial density depletions observed at 840 km during the great magnetic storm of March 1989, *J. Geophys. Res.*, *96*, 13,931–13,942.
- Hanson, W. B., and R. J. Moffett (1966), Ionization transport effects in equatorial *F* region, *J. Geophys. Res.*, *71*, 5559–5572.
- Mannucci, A. J., B. D. Wilson, D. N. Yuan, C. H. Ho, U. J. Lindqwister, and T. F. Runge (1998), A global mapping technique for GPS-derived ionospheric total electron content measurements, *Radio Sci.*, *33*, 565–582.
- Mannucci, A. J., B. A. Iijima, U. J. Lindqwister, X. Pi, L. Sparks, and B. D. Wilson (1999), GPS and ionosphere, in *Reviews of Radio Sci.*, 1996–1999, edited by W. R. Stone, Oxford Univ. Press, New York.
- Nopper, R. W., and R. L. Carovillano (1978), Polar-equatorial coupling during magnetically active periods, *Geophys. Res. Lett.*, *5*, 699–702.
- Prolss, G. W. (1997), Magnetic storm associated perturbations of the upper atmosphere, in *Magnetic Storms, Geophys. Monogr. Ser.*, vol. 98, edited by B. T. Tsurutani et al., pp. 227–241, AGU, Washington, D. C.
- Richmond, A. D. (1995), Ionospheric electrodynamics using magnetic apex coordinates, *J. Geomagn. Geoelectr.*, *47*, 191–212.
- Richmond, A. D., and G. Lu (2000), Upper-atmospheric effects of magnetic storms: A brief tutorial, *J. Atmos. Sol. Terr. Phys.*, *62*, 1115–1127.
- Skoug, R. M., J. T. Gosling, J. T. Steinberg, D. J. McComas, C. W. Smith, N. F. Ness, Q. Hu, and L. F. Burlaga (2004), Extremely high speed solar wind: 29–30 October 2003, *J. Geophys. Res.*, *109*, A09102, doi:10.1029/2004JA010494.
- Tanaka, T., and K. Ohtaka (1996), Ionospheric disturbances during low-latitude auroral events and their association with magnetospheric processes, *J. Geophys. Res.-Space Physics*, *101*(A8), 17,151–17,159.
- Tsurutani, B. T., et al. (2004), Global dayside ionospheric uplift and enhancement associated with interplanetary electric fields, *J. Geophys. Res.*, *109*, A08302, doi:10.1029/2003JA010342.
- Tsurutani, B. T., et al. (2005), The October 28, 2003 extreme EUV solar flare and resultant extreme ionospheric effects: Comparison to other Halloween events and the Bastille Day event, *Geophys. Res. Lett.*, *32*, L03S06, doi:10.1029/2004GL021502.
- Vlasov, M., M. C. Kelley, and H. Kil (2003), Analysis of ground-based and satellite observations of *F*-region behavior during the great magnetic storm of July 15, 2000, *J. Atmos. Sol. Terr. Phys.*, *65*, 1223–1234.

W. D. Gonzalez and F. L. Guarnieri, Instituto de Pesquisas Espaciais, 12201-970, São José dos Campos, CP 515, SP, Brazil.

B. A. Iijima, A. Komjathy, A. J. Mannucci, and B. T. Tsurutani, Jet Propulsion Laboratory, California Institute of Technology, 4800 Oak Grove Drive, Pasadena, CA 91109, USA. (tony.mannucci@jpl.nasa.gov)

J. U. Kozyra, Department of Atmospheric, Oceanic and Space Sciences, University of Michigan, Ann Arbor, MI 48109-2143, USA.

A. Saito, Department of Geophysics, Kyoto University, Kyoto 606-8502, Japan.

R. Skoug, Los Alamos National Laboratory, Los Alamos, NM 87545, USA.